Fig. 1b - Source gel data

p53/Drp1 axis during lytic HHV-6A infection in HSB-2 cell

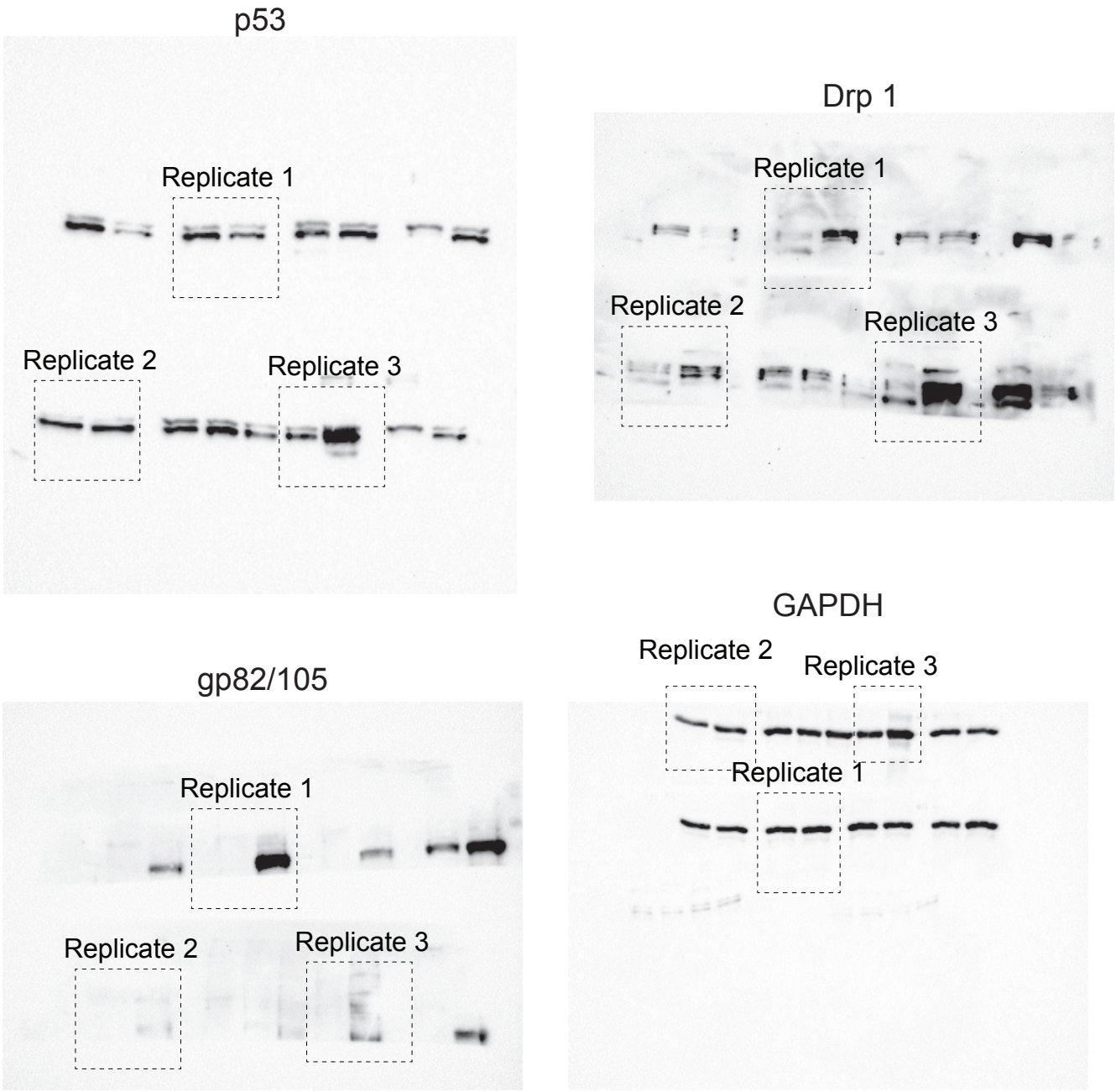

Supplementary Figure 1. Source data gels corresponding to Fig. 1b.
HSB-2 cells were either mock infected or with HHV-6A. Two days post infection, protein expression was studied by immunoblotting. HHV-6A infection of cells was confirmed using an antibody against the viral glycoprotein gp82/105. GAPDH was used as a loading control.

Fig. 1c, Extended data Fig. 2a - Source gel data

miR-30 expression during lytic HHV-6A infection in HSB-2 cell

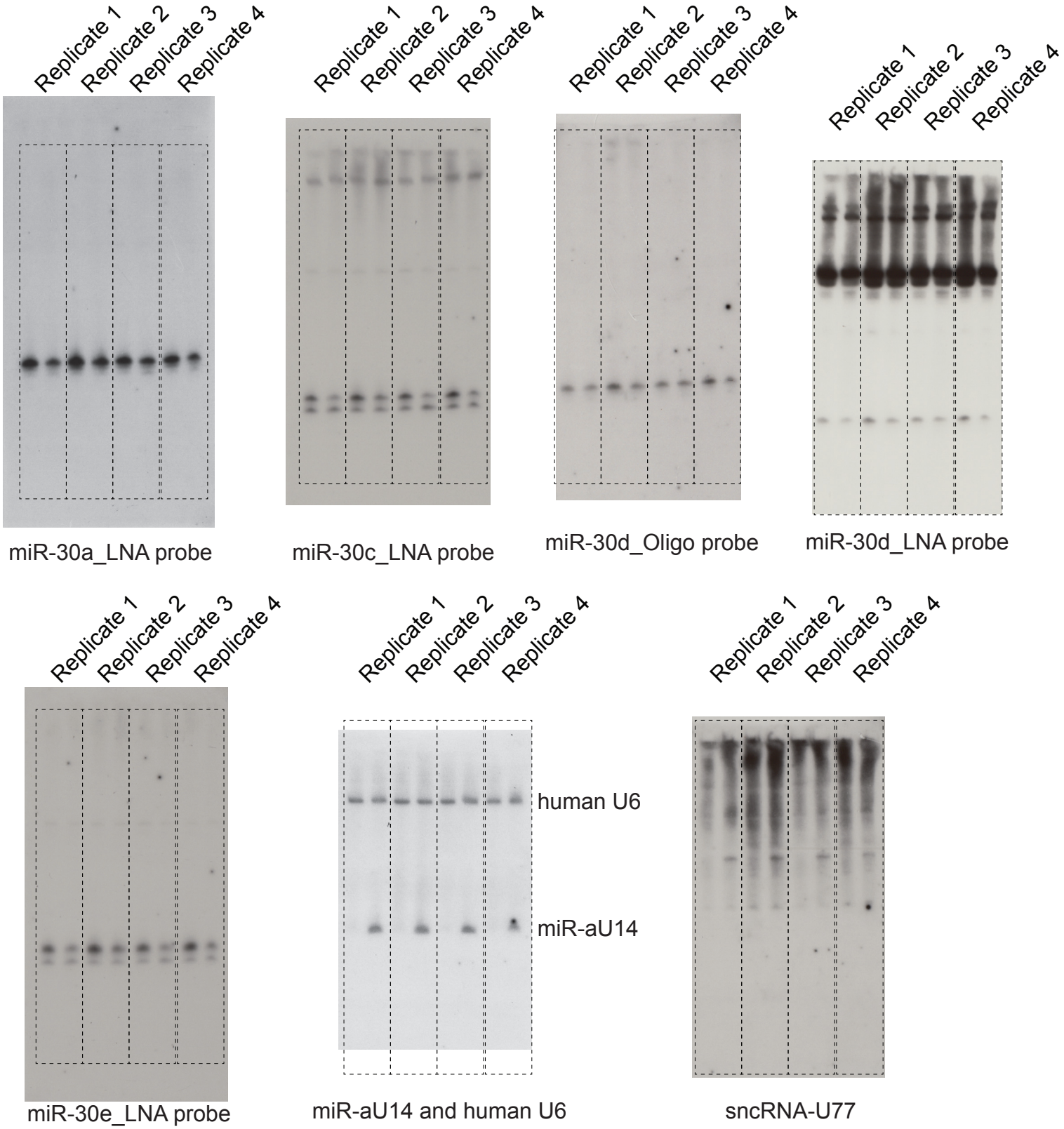

Supplementary Figure 2. Source data gels corresponding to Fig. 1c and Extended data Fig. 2a. HHV-6A infection induces processing defect of multiple miR-30 family members in HSB-2 T-cells. HSB-2 cells were infected for 48 h with HHV-6A. Total RNA from mock- and HHV-6A-infected cells were analyzed by Northern blotting. The same blot was serially probed against multiple different probes after stripping.

Fig. 1d - Source gel data

miR-30c processing defect during lytic HHV-6A infection in HSB-2 cell

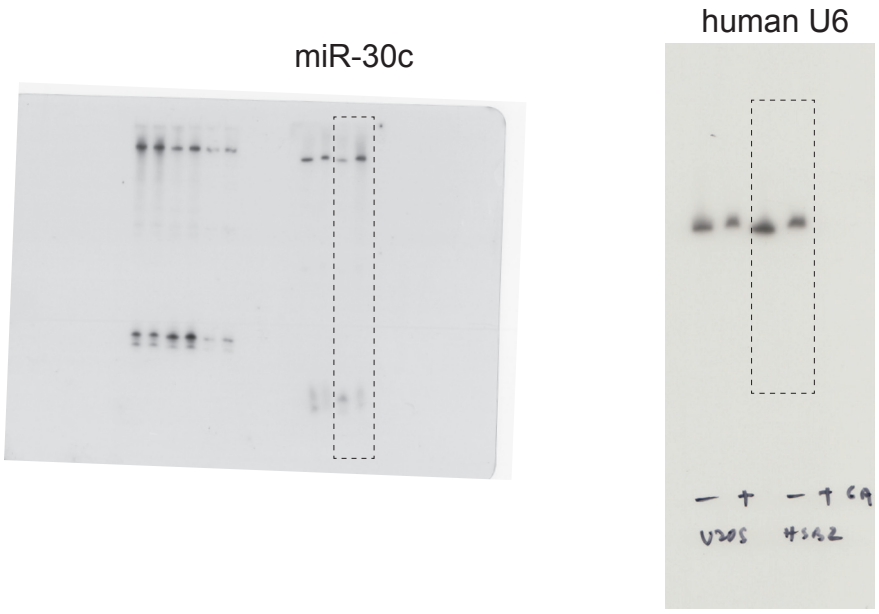

Supplementary Figure 3. Source data gels corresponding to Fig. 1d.
HHV-6A infection induces miR-30c processing defect in human HSB-2 T-cells. HSB-2 cells were infected for 48 h with HHV-6A. Total RNA from mock- and HHV-6A-infected cells were analyzed by Northern blot using LNA probes against miR-30c.

Fig. 1g - Source gel data

miR-30c processing upon transfection of miR-aU14 mimic into U2-OS cells

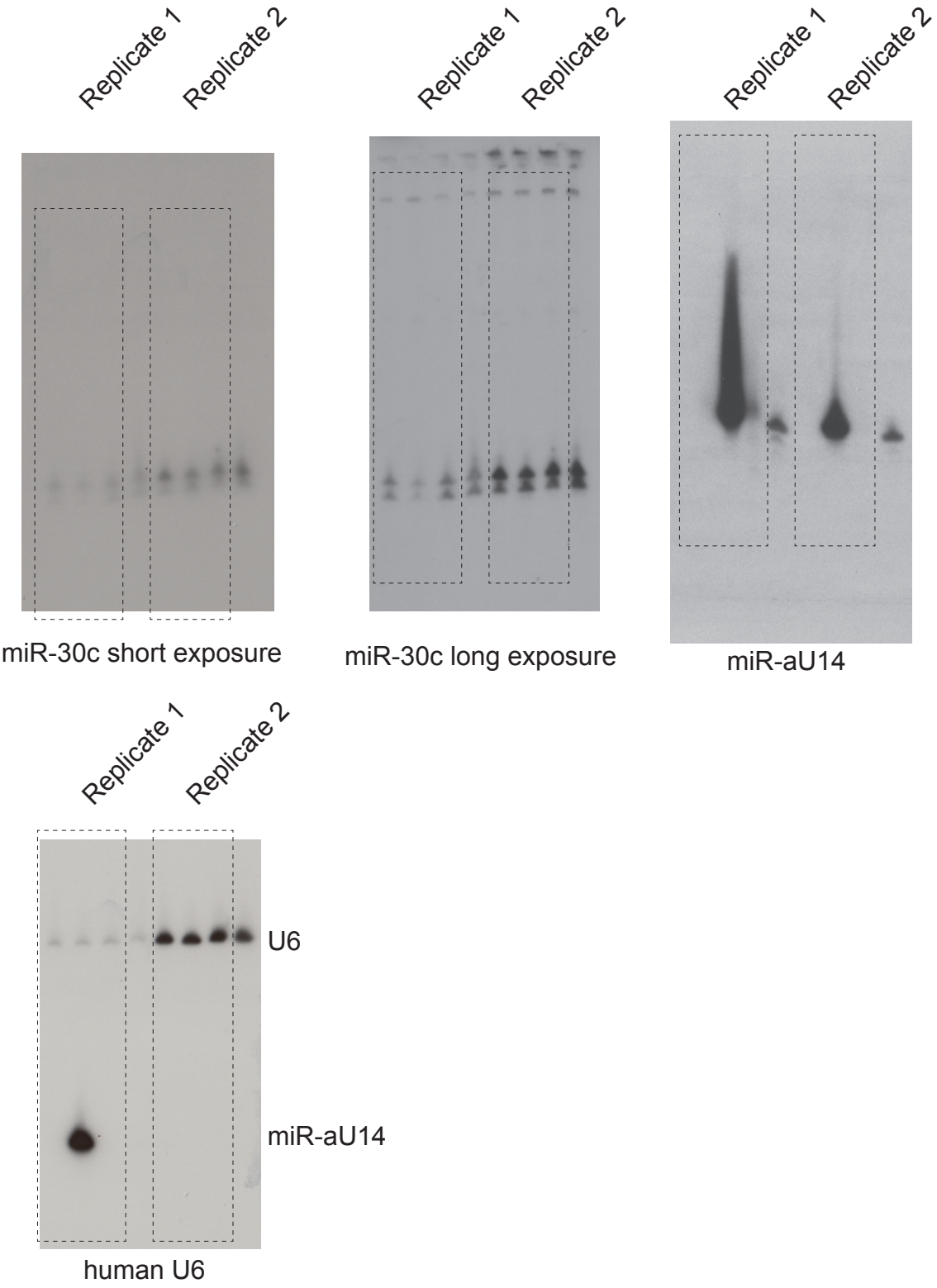

Supplementary Figure 4. Source data gels corresponding to Fig. 1g. Transfection of the wild-type but not of the mutant miR-aU14 mimic into U2-OS cells recapitulated the pri-miR-30c processing defect. U2-OS cells were transfected with the mimics for 72 h. Total RNA was exctracted and used for Northern blotting. Probe against human U6 was used as loading control.

Fig. 1h - Source gel data

miR-30c processing during lattent HHV-6A reactivation.

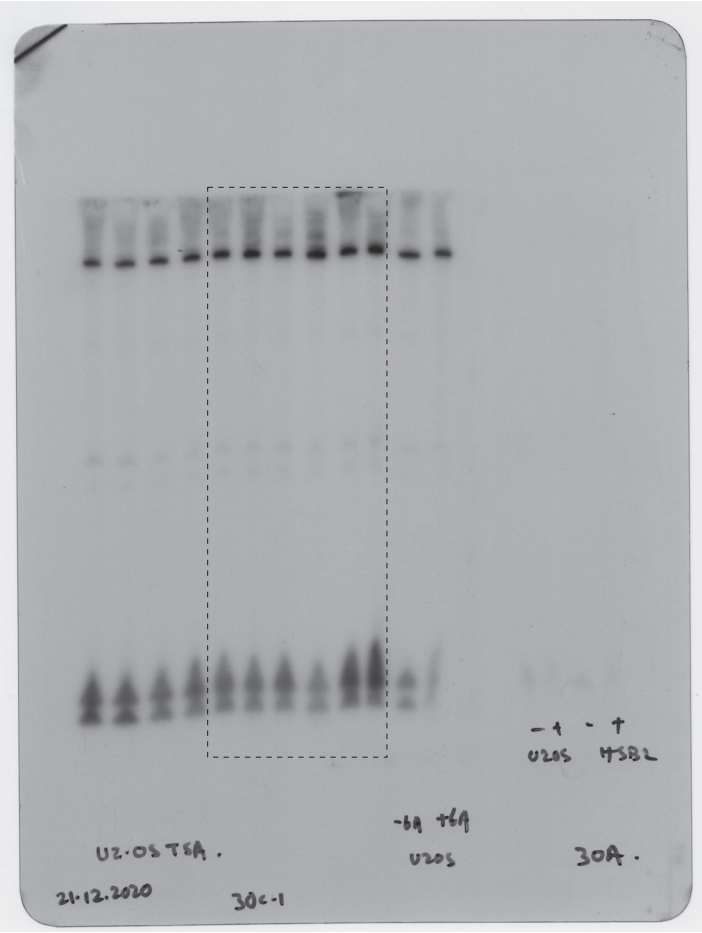

miR-30c

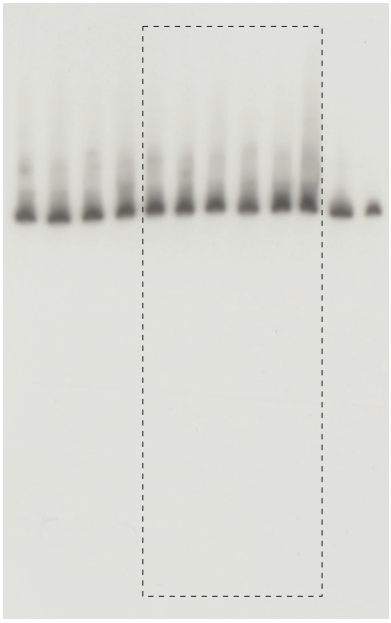

human U6

Supplementary Figure 5. Source data gels corresponding to Fig. 1h.
Reactivation of wild-type HHV-6A (HHV-6A-wt) but not of a miR-aU14 mutant virus (HHV-6A-mut) induces the pri-miR-30c processing defect. HHV-6A reactivation of U2-OS cells carrying latent wild-type or miR-aU14 mutant HHV-6A genomes was stimulated for 48 h using TSA. U2-OS cells without latent HHV-6A served as mock control. miR-30c processing was analyzed by Northern blots. Probe against human U6 was used as loading control.

Fig. 2c - Source gel data

miR-aU14 co-precipitate with biotinylated pre-miR-30c

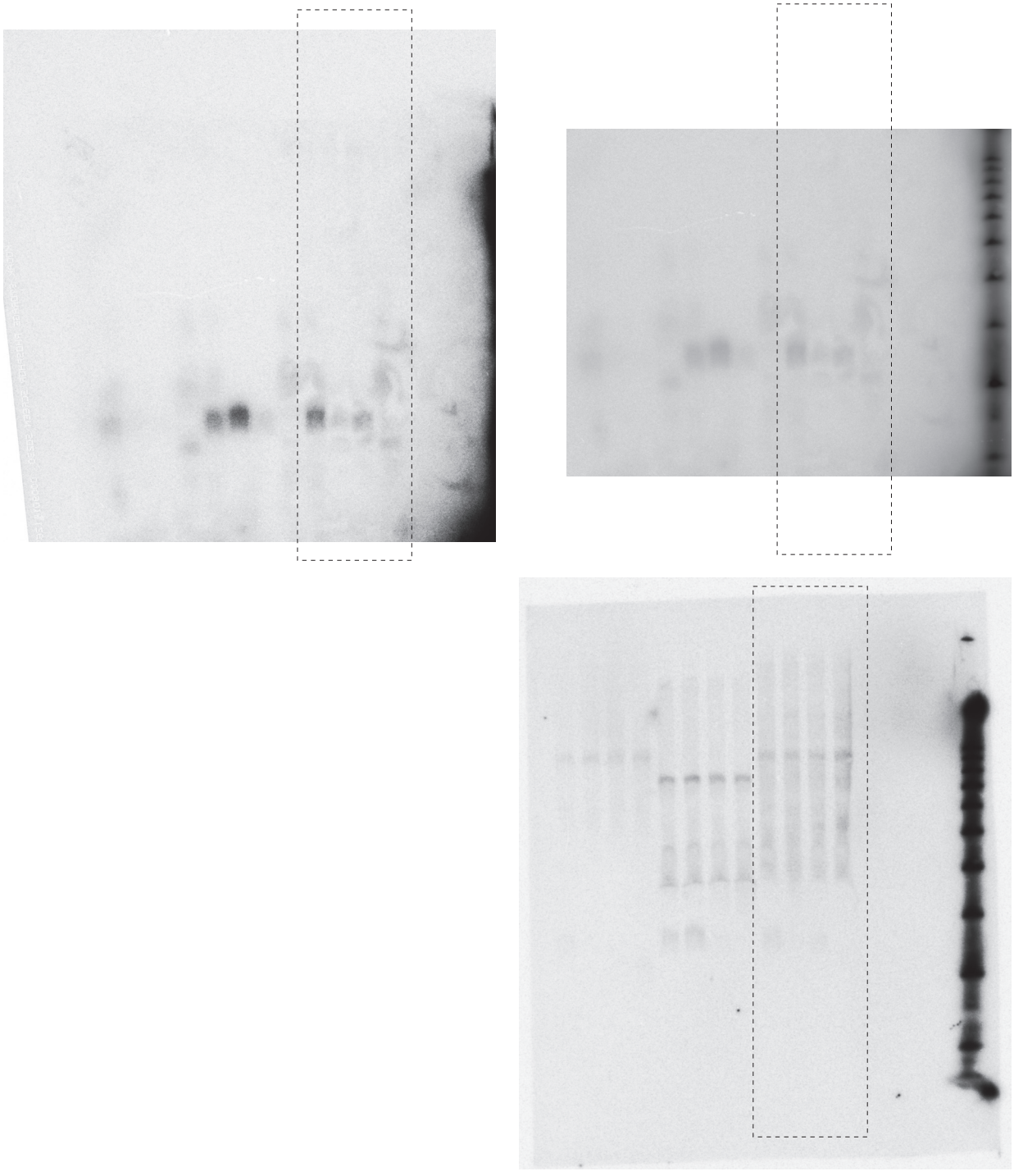

Supplementary Figure 6. Source data gels corresponding to Fig. 2c.
miR-aU14 but not its mutants co-purify with pre-miR-30c. HeLa cells were transfected with equimolar amounts of either the wild-type miR-aU14 or the two mutant sub types (Mut or Mut2) together with biotinylated pre-miR-30c RNA. 16 h post transfection, cells were sacrificed and total cell lysate was prepared for Biotin-streptavidin affinity purification. Streptavidin bead-bound RNA were used for Northern blot. A random small RNA was used as a bait for control. Purified RNA was run on a Northern blot and the membrane was directly exposed to X-ray film to detect co-purified radioactive miR-aU14. The blot was then probed for miR-30c to verify equal amounts of affinity purified biotinylated pre-miR-30c.

Fig. 2e - Source gel data

miR-aU14 impairs miRNA processing by base-pairing with the miR-30c hairpin loop.

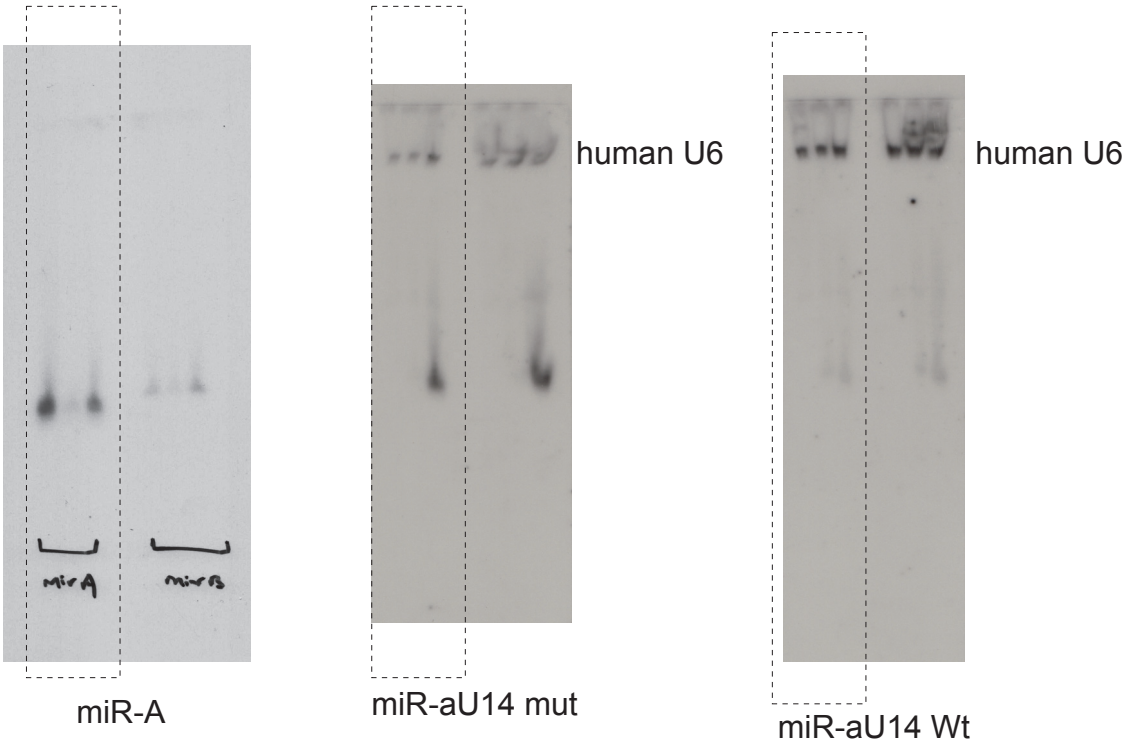

Supplementary Figure 7. Source data gels corresponding to Fig. 2e.
Polyclonal HeLa cells stably transduced for dox-inducible expression of miR-A were first selected and were subsequently re-transduced either with wild-type miR-aU14 (HeLa-Wt), mutant miR-aU14 (HeLa-Mut) or with an empty vector (HeLa-Mock). 72 h post dox-induction, total RNA was prepared and run on Northern blot. Expression of miR-A was evaluated. Probe against human U6 was used as a loading control.

Fig. 2f - Source gel data

miR-aU14 impairs miRNA processing by base-pairing with the miR-30c hairpin loop.

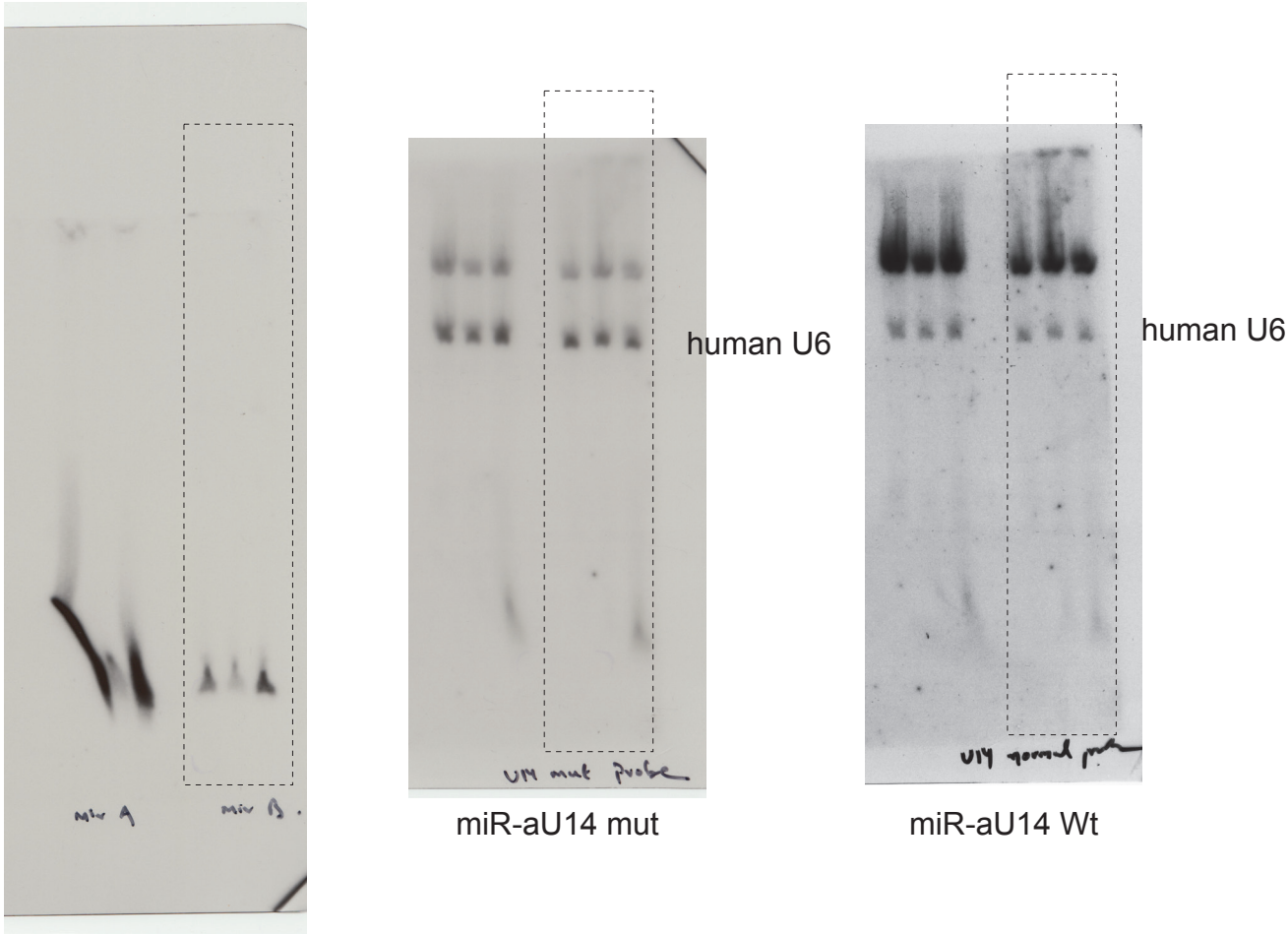

Supplementary Figure 8. Source data gels corresponding to Fig. 2f.
Polyclonal HeLa cells stably transduced for dox-inducible expression of miR-B were first selected and were subsequently re-transduced either with wild-type miR-aU14 (HeLa-Wt), mutant miR-aU14 (HeLa-Mut) or with an empty vector (HeLa-Mock). 72 h post dox-induction, total RNA was prepared and run on Northern blot. Expression of miR-B was evaluated. Probe against human U6 was used as a loading control.

Fig. 3c - Source gel data

miR-30c processing defect during lytic HHV-6A infection in HSB-2 cell

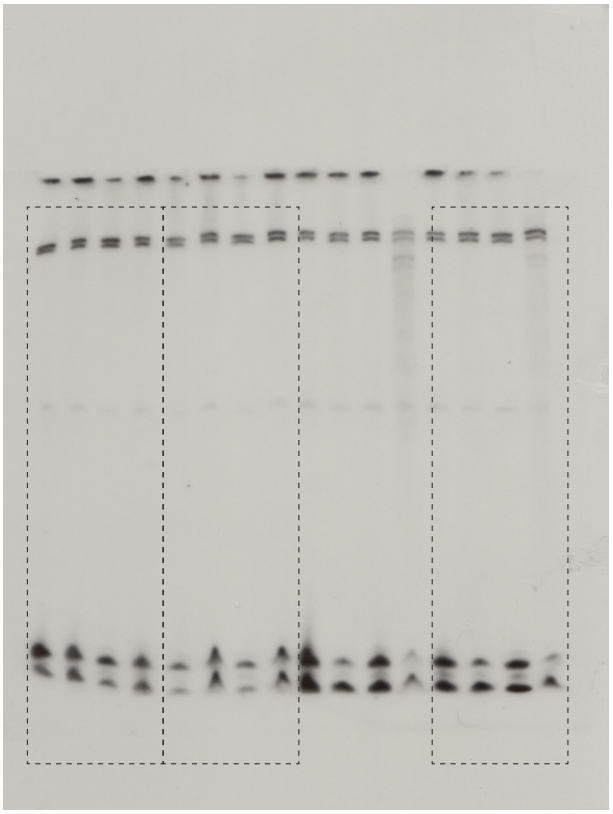

miR-30c

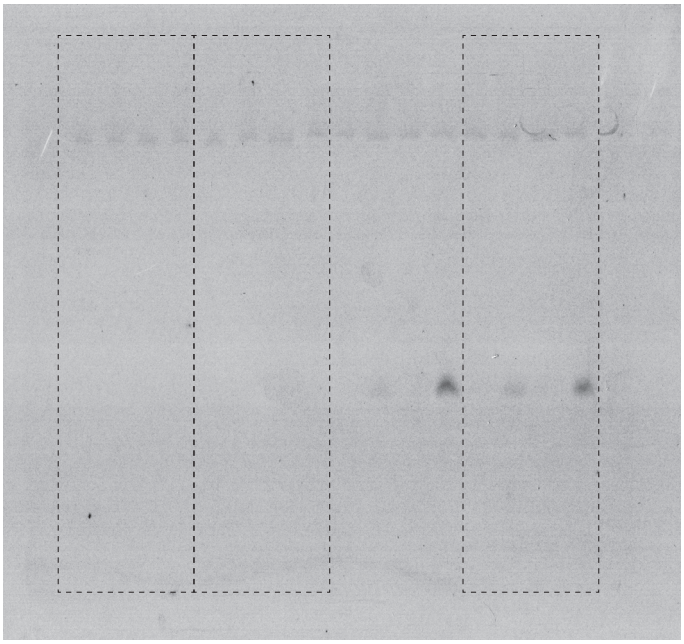

miR-aU14

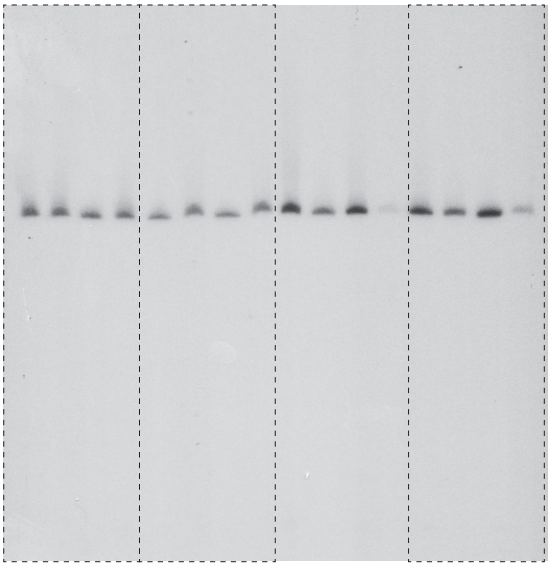

human U6

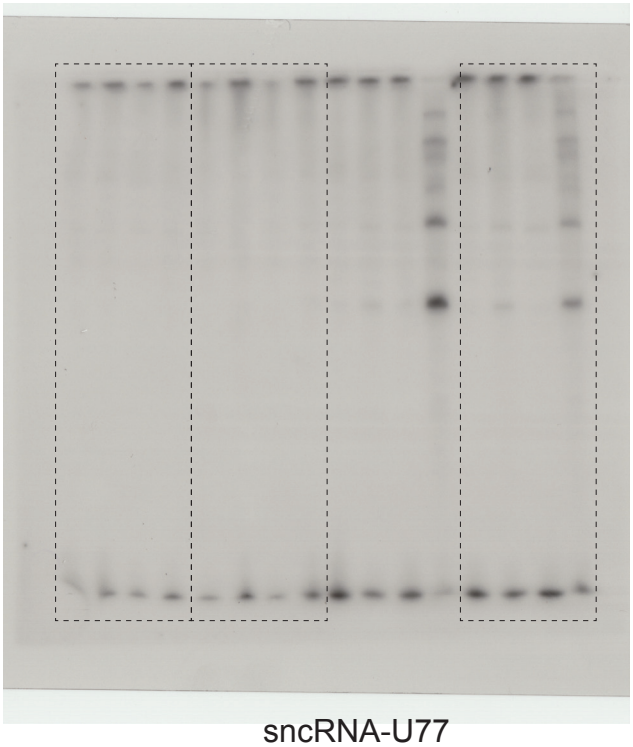

sncRNA-U77

Supplementary Figure 9. Source data gels corresponding to Fig. 3c. Reactivation of wild-type HHV-6A (HHV-6A-wt) but not the miR-aU14 mutant (HHV-6A-mut) induces a pri-miR-30c processing defect. Total RNA from TSA-treated or TSA- together with Ruxolitinib-treated U2-OS cells carrying latent HHV-6A was studied using Northern blotting. Probe against human U6 was used as loading control. U2-OS cells without latent HHV-6A served as mock control. The blot was reprobed with probes against miR-aU14 and sncRNA-U77.

Fig. 3g - Source gel data

miR-aU14 regulates virus latent/lytic switch

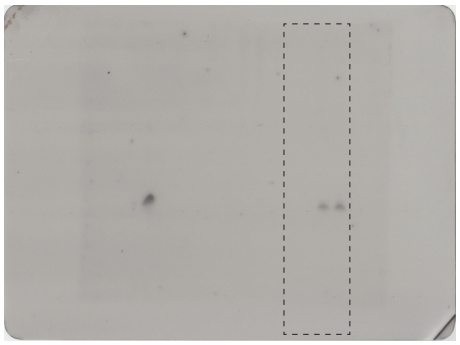

miR-U86

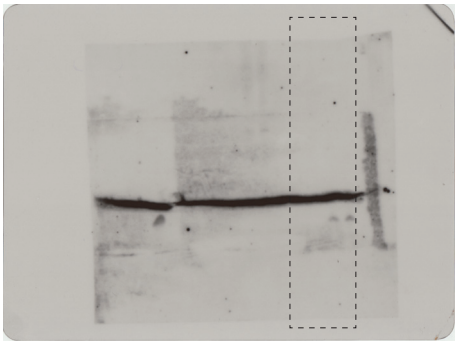

miR-U2

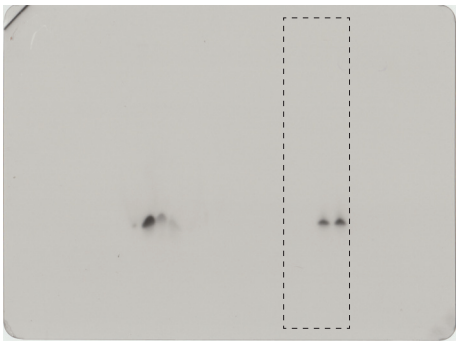

miR-aU14

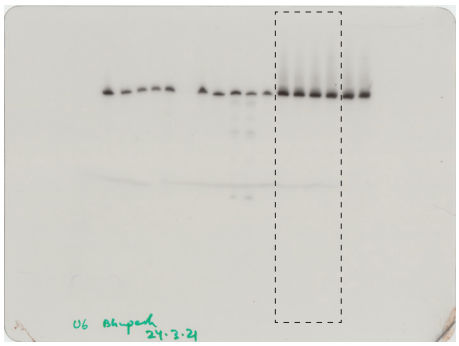

human U6

Supplementary Figure 10. Source data gels corresponding to Fig. 3g.
Effect of exogenous miR-aU14 on the reactivation of mutant HHV-6A. U2-OS cells carrying latent HHV-6A miR-aU14 mutant (HHV-6A-mut) were transfected with either the miR-aU14 mimic or a control mimic. Cells were induced with TSA and the extent of virus reactivation was analyzed by Northern blot for viral miR-U2, miR-U86. The same membrane was reprobed for various miRNAs and controls following striping. The original gel images are shown in order of their use. Probe against human U6 was used as loading control.

Fig. 4b - Source gel data

Human miRNA processing can be selectively inhibited by synthetic small RNAs

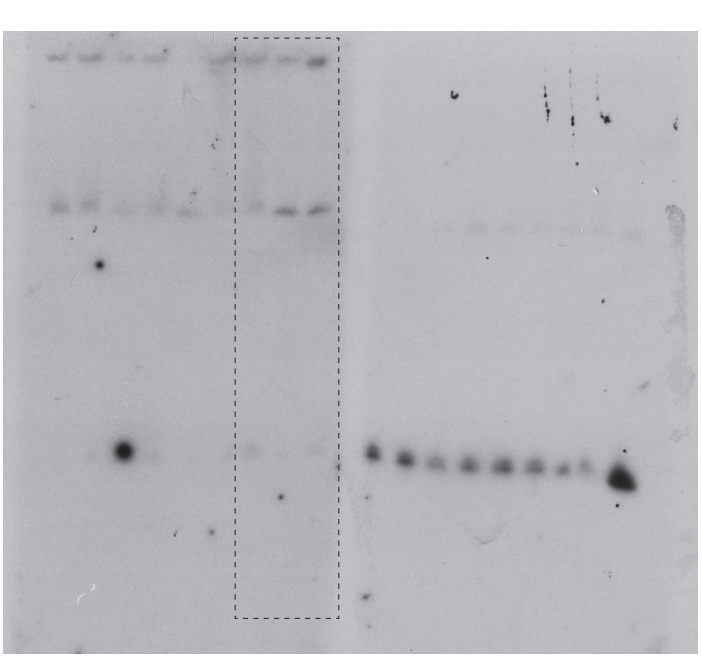

let-7d

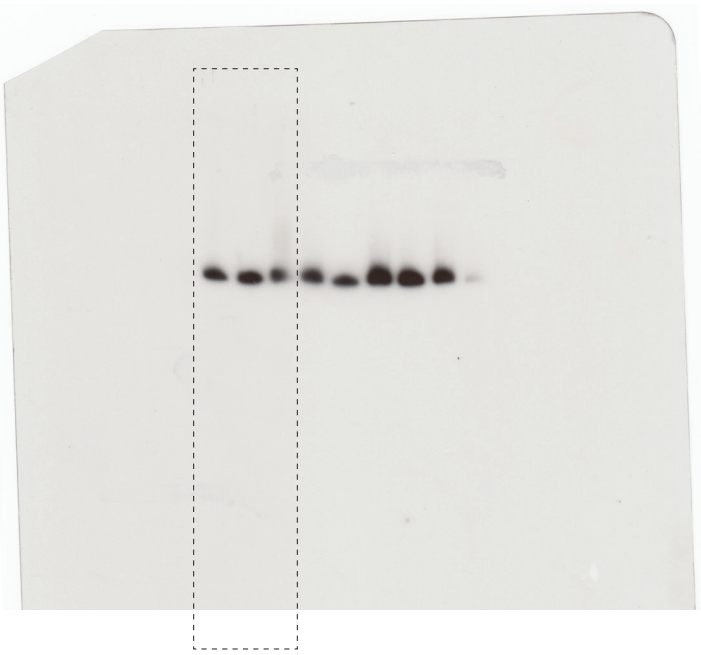

human U6

Supplementary Figure 11. Source data gels corresponding to Fig. 4b.
Targeting the hairpin loop of pre-let-7d with synthetic miRNAs interferes with miRNA processing. Two different miRNA mimics were designed against the hairpin loop of pre-let-7d and were transfected into U2-OS cells. Three days post transfection, total cellular RNA was prepared and used to study let-7d miRNA levels by Northern blotting. Probe against human U6 was used as loading control.

Fig. 4d - Source gel data

Human miRNA processing can be selectively inhibited by synthetic small RNAs

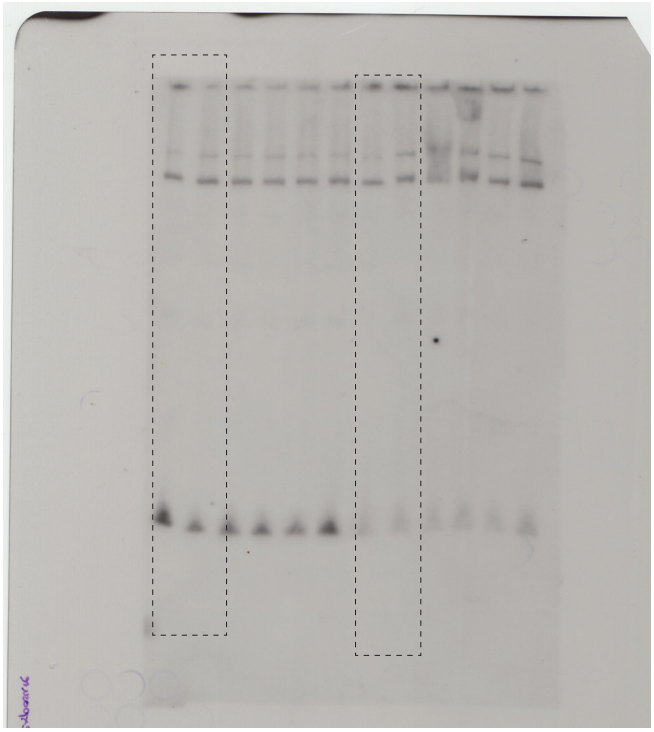

miR-148b

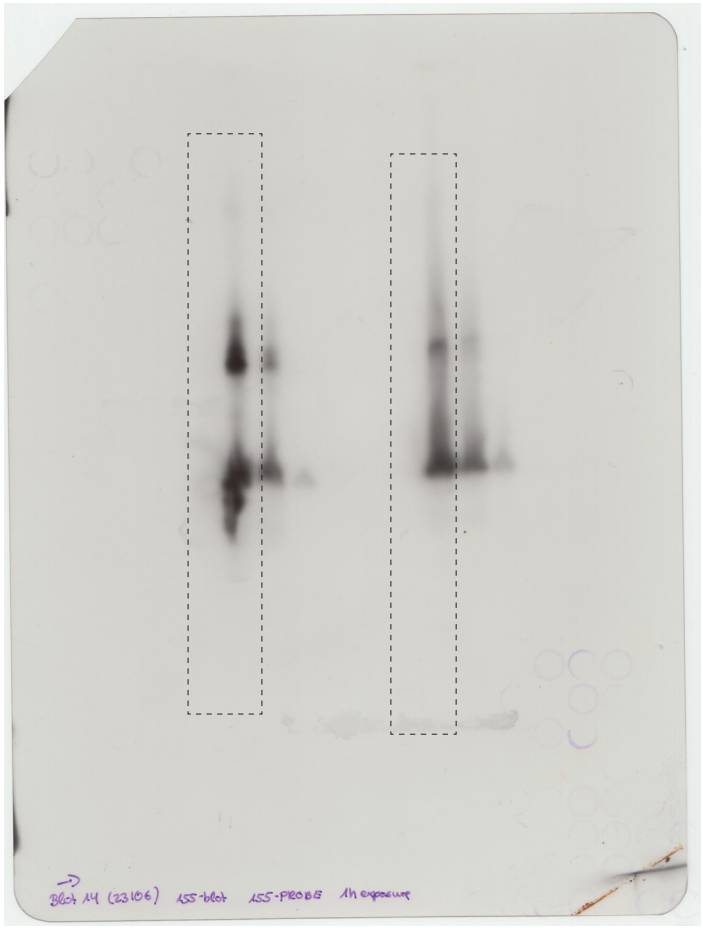

miR-155

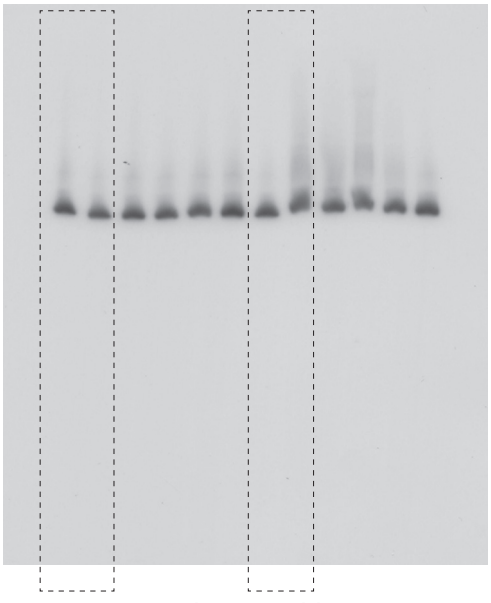

human U6

Supplementary Figure 12. Source data gels corresponding to Fig. 4d.
miR-155 interferes with pri-miR-148b processing. A synthetic miR-155 mimic was transfected for 72 h into either HEK293T or HeLa cells. Total cellular RNA was used to study miR-148b miRNA levels. Probe against human U6 was used as a loading control. Endogenous miR-155 levels are too low to be detected by Northern blotting in cells in presence of high levels of transfected mimic.

Extended data Fig. 1b - Source gel data

p53/Drp1 axis during reactivation of HHV-6A in U2-OS cells

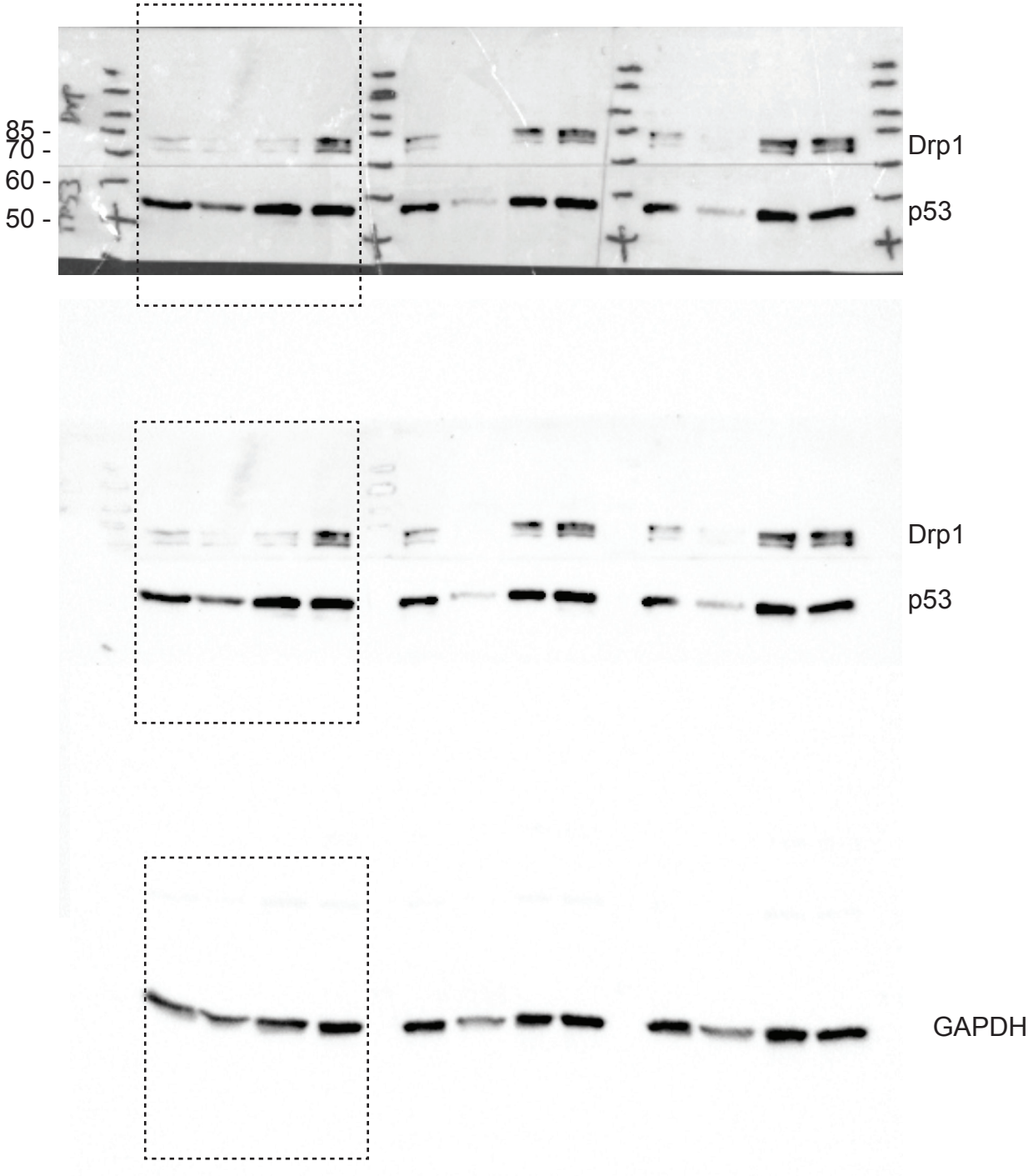

Supplementary Figure 13. Source data gels corresponding to Extended data Fig. 1b. HHV-6A reactivation increases the expression of p53 and Drp1. Virus reactivation in U2-OS cells with or without latent HHV-6A was induced for 48 h using TSA or solvent control. Changes in Drp1 and p53 protein expression were quantified using densitometric analysis of immunoblots and were normalized for GAPDH.

Extended data Fig. 2b - Source gel data

HHV-6A reactivation impairs miR-30c processing.

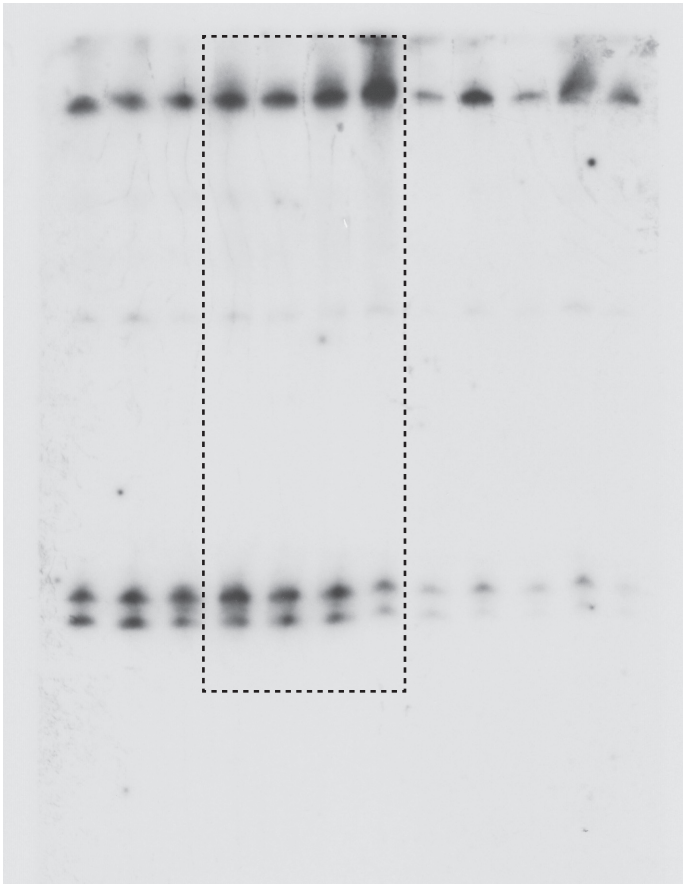

miR-30c

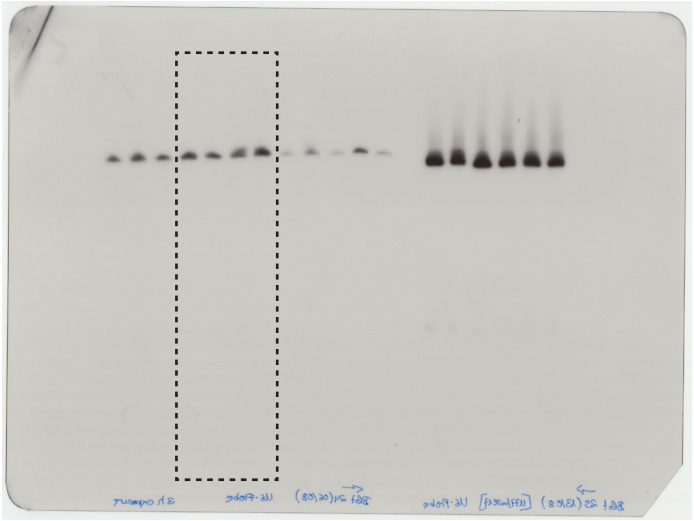

human U6

Supplementary Figure 14. Source data gels corresponding to Extended data Fig. 2b. HHV-6A reactivation induces miR-30c processing defect in U2-OS cells. Virus reactivation of U2-OS cells carrying latent HHV-6A was induced for 48 h using TSA. U2-OS cells without latent HHV-6A served as mock control. miR-30c levels were studied by Northern blotting.

Extended data Fig. 2c - Source gel data

HHV-6A reactivation impairs miR-30 processing.

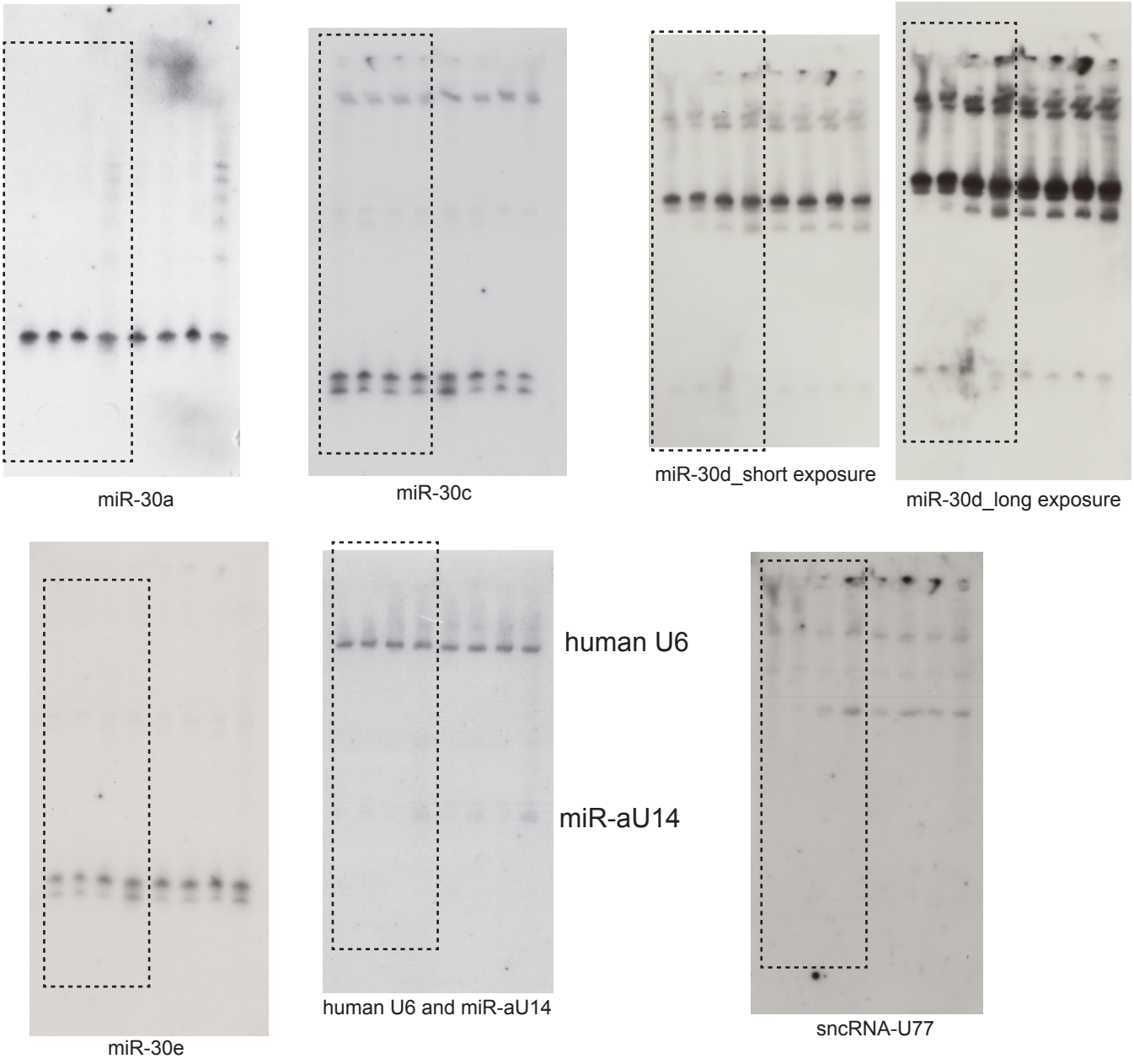

Supplementary Figure 15. Source data gels corresponding to Extended data Fig. 2c. HHV-6A reactivation induces miR-30 processing defect in U2-OS cells. Virus reactivation of U2-OS cells carrying latent HHV-6A was induced for 48 h using TSA. U2-OS cells without latent HHV-6A served as mock control. miR-30 levels were studied by Northern blotting. Images for human U6 loading control, miR-aU14 and sncRNA-U77 are the same as the blots were stripped and used for reprobing against multiple miR-30 family members. All the images shown are from a single gel.

Fig. 5b - Source gel data

Inducible miR-aU14 expression in HeLa cells induce miR-30c processing defect.

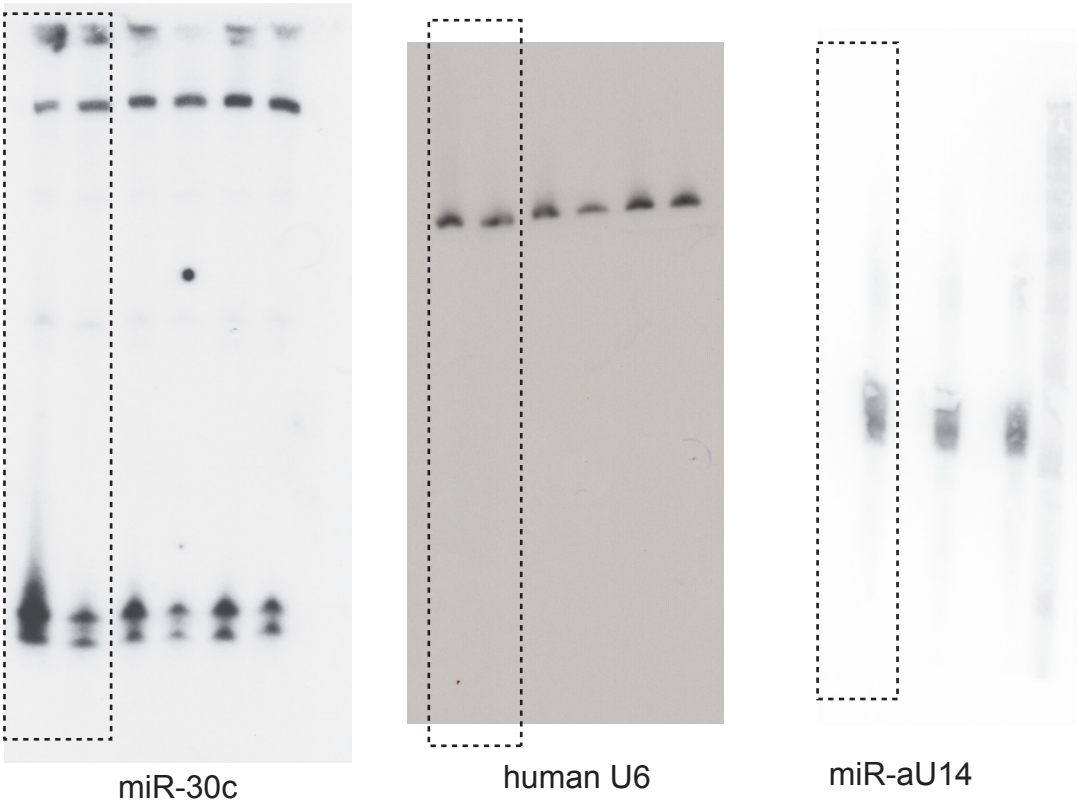

Supplementary Figure 16. Source data gels corresponding to Extended data Fig. 5b. Doxycycline (dox)-inducible miR-aU14 inhibits miR-30c processing. HeLa cells were stably transduced to express dox-inducible miR-aU14. Polyclonal cells were induced by dox for 48 h. miR-30c and miR-aU14 expression was probed by Northern blotting. Probe against human U6 served as loading control.

Fig. 5c - Source gel data

Inducible miR-aU14 expression in HeLa cells induce miR-30c processing defect.

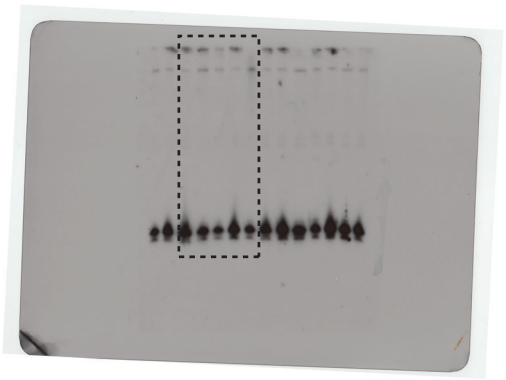

miR-30c

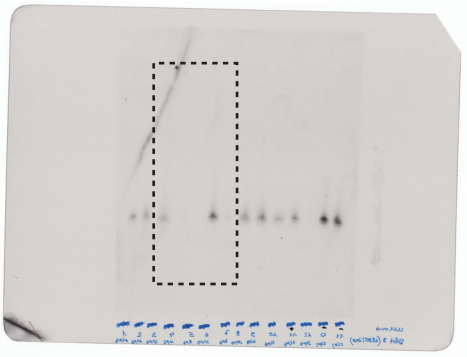

Mutant miR-aU14

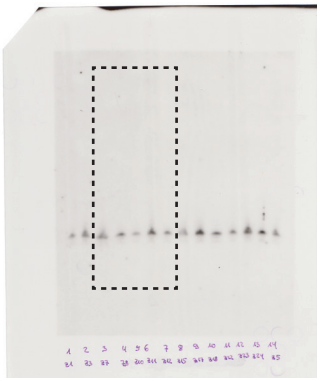

Wild type miR-aU14

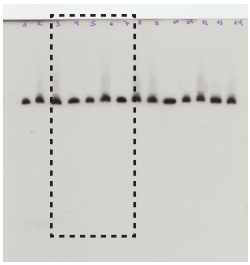

miR-aU14

Supplementary Figure 17. Source data gels corresponding to Extended data Fig. 5c. Dox-inducible wild-type but not mutant miR-aU14 inhibits miR-30c processing. Polyclonal HeLa cells stably transduced to express either wild-type (HeLa-Wt1, 2 and 3) or mutant (HeLa-Mut1 and 2) miR-aU14 were induced by dox for 48 h. Multiple batches of polyclonal cells were analyzed in parallel for comparison. miR-30c and miR-aU14 expression were probed by Northern blotting. Probe against human U6 was used as loading control.

Fig. 5d - Source gel data

miR-aU14 mimic induces Drp1 and p53 expression.

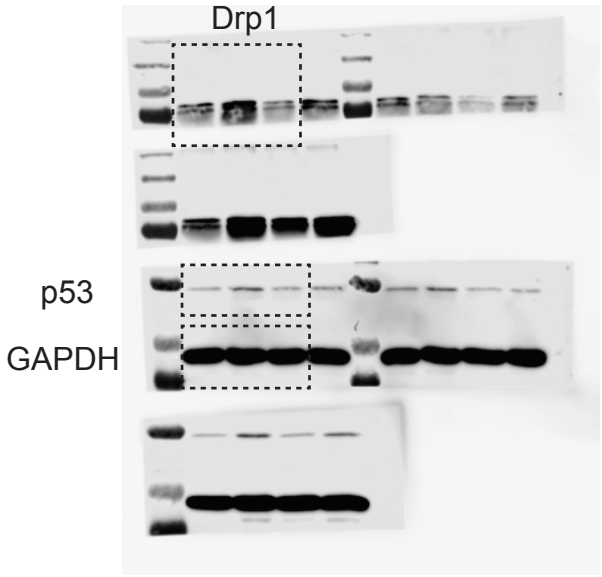

Supplementary Figure 18. Source data gels corresponding to Extended data Fig. 5d. Transfection of miR-aU14 mimic induces Drp1 and p53 protein expression in U2-OS cells. Total protein lysates from cells transfected for 48 h with either a control mimic, miR-aU14 mimic (Wt mimic), or the mutant miR-aU14 mimic (Mut mimic) were subjected to immunoblot analysis.

Fig. 5e - Source gel data

Inducible expression of miR-aU14 induces Drp1 expression.

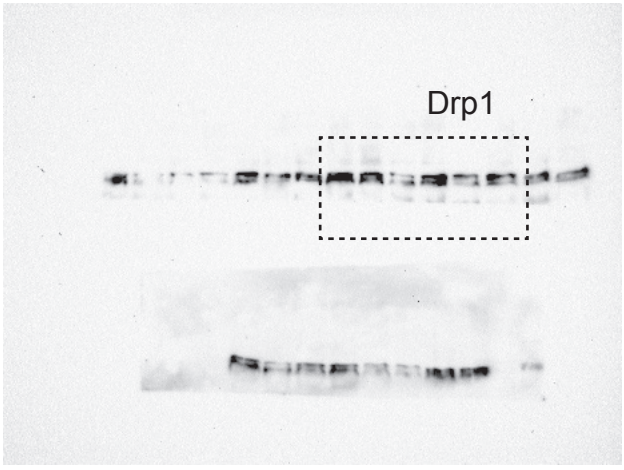

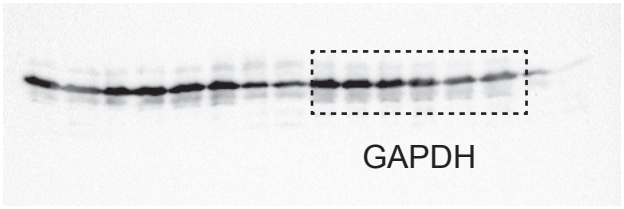

Supplementary Figure 19. Source data gels corresponding to Extended data Fig. 5e. Dox-inducible expression of miR-aU14 in HeLa cells induced Drp1 expression. Polyclonal HeLa cells with dox-inducible wild-type (HeLa-Wt) or mutant miR-aU14 (HeLa-Mut) were stimulated by dox for 72 h. Non-transduced HeLa cells served as controls. Total protein lysates were subjected to immunoblot analysis.

Fig. 6b - Source gel data

HHV-6A with wild type miR-aU14 but not the mutant induces Drp1 expression during virus reactivation.

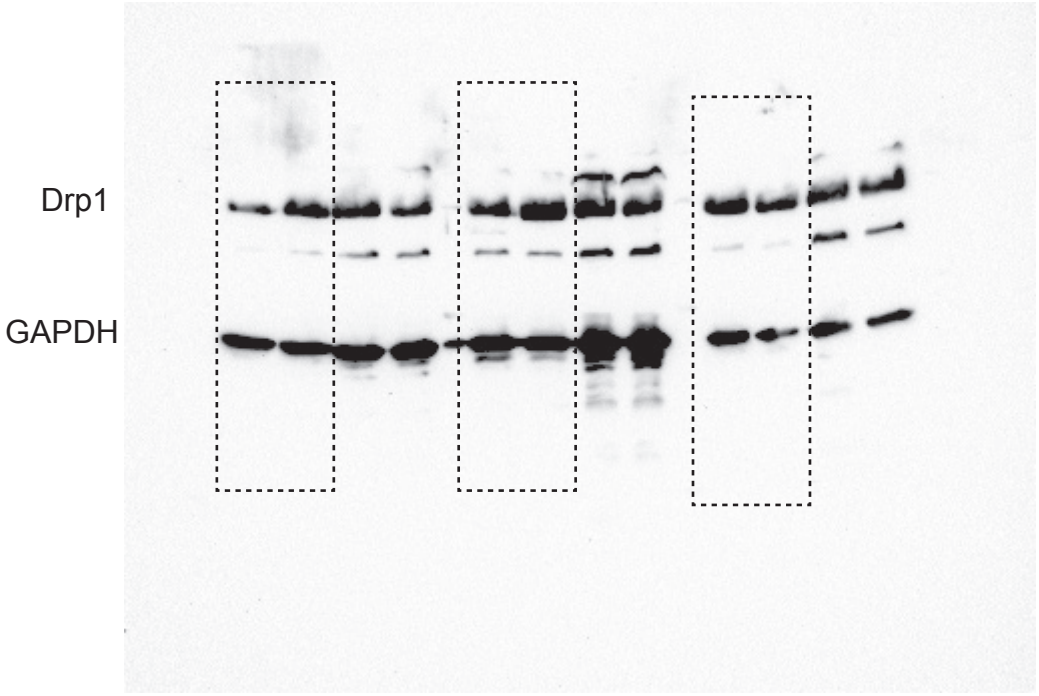

Supplementary Figure 20. Source data gels corresponding to Extended data Fig. 6b. Reactivation of wild-type but not mutant HHV-6A induces Drp1 expression. HHV-6A reactivation of U2-OS cells carrying latent wild-type (HHV-6A-wt) or miR-aU14 mutant (HHV-6A-mut) HHV-6A genomes was stimulated for 48 h using TSA. U2-OS cells without latent HHV-6A served as mock control. Total protein lysates were subjected to immunoblot analysis.

Extended data Fig. 7a - Source gel data

miR-aU14 regulates virus latent/lytic switch in wild type HHV-6A carrying cells

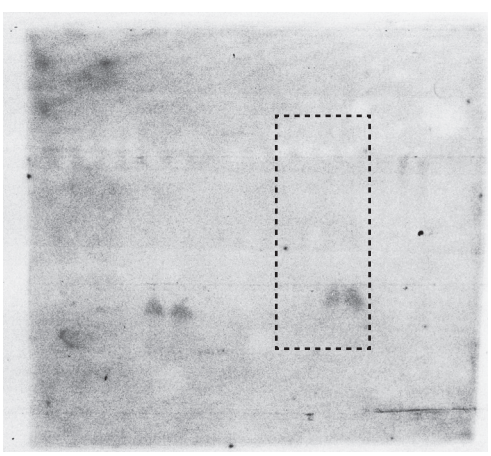

miR-U86

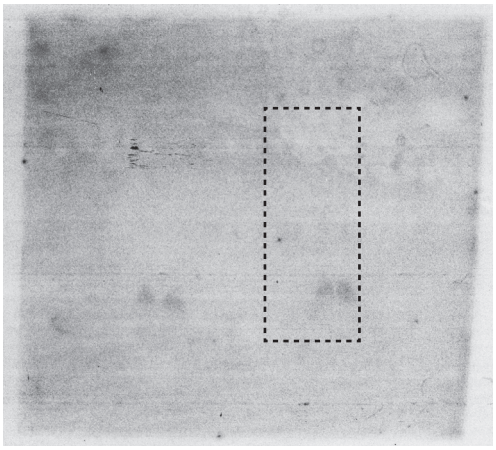

miR-U2

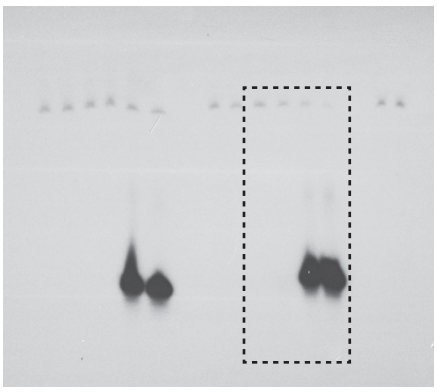

miR-aU14

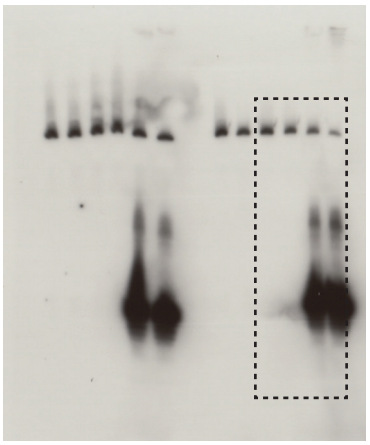

human U6

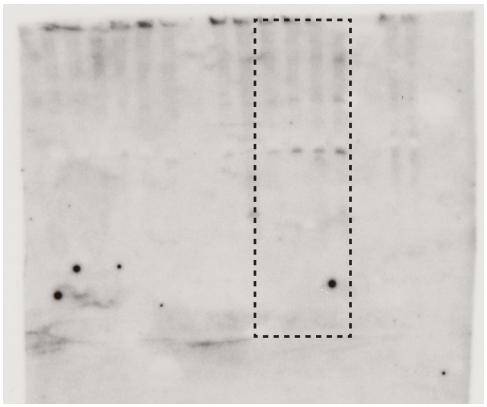

sncRNA-U77

Supplementary Figure 21. Source data gels corresponding to extended data Fig. 7a. Effect of exogenous miR-aU14 on the reactivation of wild-type HHV-6A (HHV-6A-wt). U2-OS cells carrying latent wild-type HHV-6A were transfected with miR-aU14 mimic or a control mimic. Cells were induced with TSA and the extent of virus reactivation was analyzed by Northern blot for viral miR-U2, miR-U86, sncRNA-U77. Probe against human U6 was used as loading control.

Extended data Fig. 7b - Source gel data

miR-aU14 regulates virus latent/lytic switch in wild type HHV-6A carrying cells

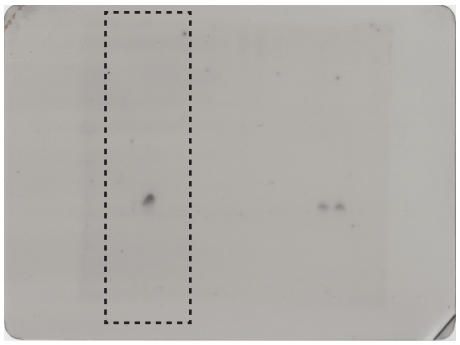

miR-U86

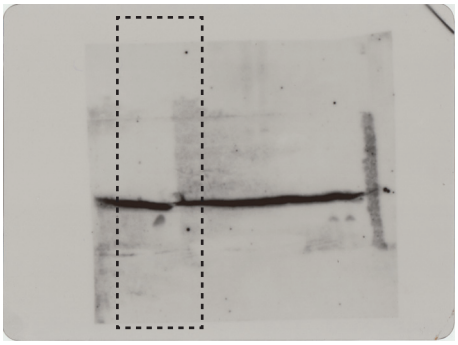

miR-U2

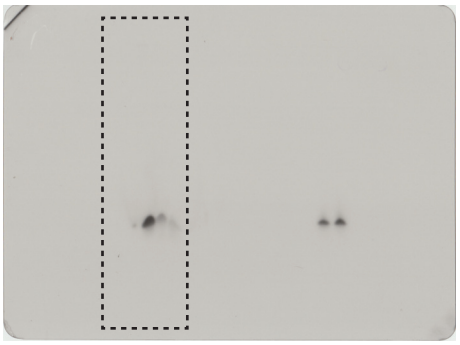

miR-aU14

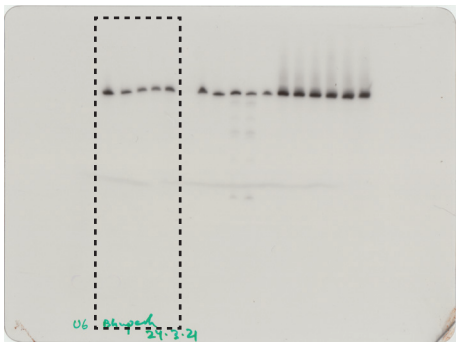

human U6

Supplementary Figure 22. Source data gels corresponding to extended data Fig. 7b. Effect of exogenous miR-aU14 on the reactivation of wild-type HHV-6A (HHV-6A-wt). U2-OS cells carrying latent wild-type HHV-6A were transfected with either the miR-aU14 mimic or two mutant miRNA mimics. Cells were induced with TSA and the extent of virus reactivation was analyzed by Northern blot for viral miR-U2, miR-U86. The same membrane was reprobed for various miRNAs and controls following striping. The original gel images are shown in order of their use.Probe against human U6 was used as loading control.

Extended data Fig. 8b - Source gel data

Human let-7f1 processing can be selectively inhibited by synthetic small RNAs.

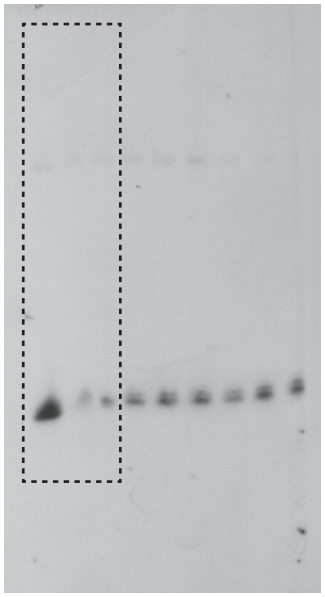

let-7f1

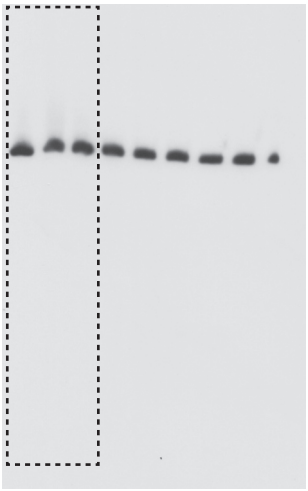

human U6

Supplementary Figure 23. Source data gels corresponding to extended data Fig. 8b. Targeting the hairpin loop of pre-let-7f1 with synthetic miRNAs interferes with miRNA processing. Two different miRNA mimics were designed against the hairpin loop of pre-let-7f1 and were transfected into U2-OS cells. Three days post transfection, total cellular RNA was prepared and used to study let-7f1 miRNA levels by Northern blotting. Probe against human U6 was used as loading control.